Label-Free, Electrical Detection of the SARS Virus N-Protein with Nanowire Biosensors Utilizing Antibody Mimics as Capture Probes

Fumiaki N. Ishikawa,[†] Hsiao-Kang Chang,[†] Marco Curreli,[‡] Hsiang-I Liao,[⊥] C. Anders Olson,[‡] Po-Chiang Chen,[†] Rui Zhang,[‡] Richard W. Roberts,[‡] Ren Sun,[⊥] Richard J. Cote,[§] Mark E. Thompson,[‡,*] and Chongwu Zhou[†,*]

[†]Departments of Electrical Engineering, [‡]Chemistry, and [§]Pathology, University of Southern California, Los Angeles, California 90089, and [⊥]Department of Molecular and Medical Pharmacology, University of California Los Angeles, Los Angeles, California 90095

ABSTRACT Antibody mimic proteins (AMPs) are polypeptides that bind to their target analytes with high affinity and specificity, just like conventional antibodies, but are much smaller in size (2−5 nm, less than 10 kDa). In this report, we describe the first application of AMP in the field of nanobiosensors. In_2O_3 nanowire based biosensors have been configured with an AMP (Fibronectin, Fn) to detect nucleocapsid (N) protein, a biomarker for severe acute respiratory syndrome (SARS). Using these devices, N protein was detected at subnanomolar concentration in the presence of 44 μM bovine serum albumin as a background. Furthermore, the binding constant of the AMP to Fn was determined from the concentration dependence of the response of our biosensors.

KEYWORDS: biosensor · nanowire · nucleocapsid (N) protein · antibody mimetic protein

In less than a decade, biosensors based on nanowire/carbon nanotube transistors have successfully made the transition from proof of concept[1] to highly selective, ultrasensitive devices capable of detecting specific proteins and DNA sequences.[2−8] These devices utilize a capture agent on the sensor surface to selectively bind the target biomolecules. The captured biomolecules affect the electronic properties of the nanowires/nanotubes, resulting in an electronically readable signal. Capture agents commonly used in nanobiosensors include antibodies, oligonucleotides, and small ligands (*e.g.*, biotin).[1−4,8]

Antibody mimic proteins (AMPs) are a class of affinity binding agents developed by *in vitro* selection techniques.[9,10] These AMPs can be evolved/engineered to improve recognition properties such as selectivity and binding affinity, with the potential to surpass antibodies and nucleotide aptamers. In contrast to typical antibodies, AMPs are stable to a wide range of pH and electrolyte concentrations, and are relatively small (usually 2−5 nm, less than 10 kDa). Moreover, it is expected that these peptide based affinity agents can be produced in large quantity, at relatively low cost. The combination of low cost, high binding affinity, chemical stability, and small size makes AMPs particularly attractive for use with nanowire/nanotube biosensors.

In this report, we introduce evolved AMPs as a new class of capture agents for nanowire/nanotube biosensors. These AMPs will allow us to build nanobiosensors for virtually any biomolecule with high sensitivity/selectivity, as demonstrated here for a protein related to severe acute respiratory syndrome (SARS), using devices based on In_2O_3 nanowires. Metal oxide nanowires, such as In_2O_3, ZnO, and SnO_2, can be easily derivatized and their surface do not possess an insulating, native oxide layer (*e.g.*, SiO_2 on Si nanowires) that may decrease the nanowire sensitivity.[8] Thus, it is worthwhile to investigate metal oxide nanowires as alternative nanomaterials to silicon nanowires for biosensing applications. We demonstrate that our technology platform, entailing In_2O_3 nanowire FETs combined with AMPs, can be used as a diagnostic tool with the potential to serve as a cost-effective, rapid, portable system. A fibronectin-based protein (Fn) was employed as an example of AMP capture agent to selectively recognize and bind the nucleocapsid (N) protein. The N protein is a biomarker associated with the SARS coronavirus.[11] Our platform is

*Address correspondence to chongwuz@usc.edu, met@usc.edu.

Received for review January 29, 2009 and accepted April 15, 2009.

Published online May 7, 2009.
10.1021/nn900086c CCC: $40.75

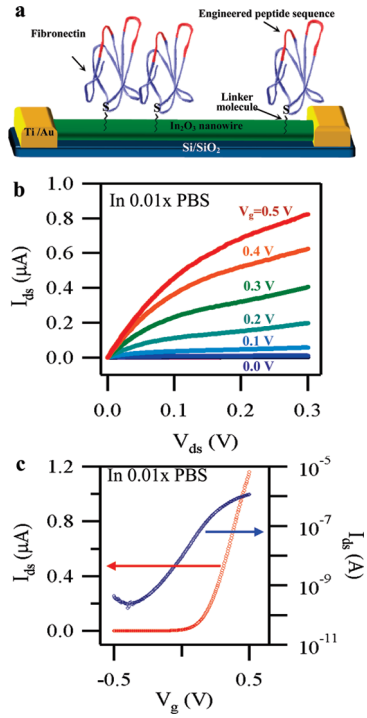

Figure 1. (a) Schematic diagram showing Fn immobilized on the surface of an In_2O_3 nanowire FET device. The regions of Fn with the engineered peptide sequence are highlighted in red. Fn was attached to the NWs *via* the sulfydryl group of a cysteine near the C-terminus, remote from the binding site. (b) A family of $I_{ds}-V_{ds}$ curves and (c) a typical $I_{ds}-V_g$ curve (plotted both in linear (red) and logarithmic (blue)) obtained from one of our devices operating with the liquid gate configuration.

capable of specifically detecting the N protein at subnanomolar concentrations, in the presence of 44 μM bovine serum albumin (BSA) as a background. This sensitivity, while comparable to current immunological detection methods, can be obtained in a relatively short time and without the aid of any signal amplifier, such as fluorescence labeled reagents. Ultimately, we show that our platform can also be used to accurately determine the dissociation constant of the N protein and Fn by applying a conventional Langumir model to the concentration-dependent sensing response.

RESULTS AND DISCUSSION

A schematic illustration of our fibronectin-based capture agent anchored to an In_2O_3 nanowire field-effect transistor is shown in Figure 1a. Our Fn-based AMP was evolved using mRNA display from a large library of potential candidates and possesses a high binding affinity to the N protein (K_D = 3.3 nM), as described in details elsewhere.[12] The evolved portion of N-protein is highlighted in red in Figure 1a. Our Fn probe was also engineered to have a single cystine residue near the C-terminus of the protein, remote from the binding site (Figure 1a and Supporting Information Figure S1). This unique thiol group allows the Fn anchoring to the nanowire to be carried out selectively, since the chosen linker molecule/chemistry (*i.e.*, maleimide groups) gives a nanowire surface that is reactive only toward sulfydryl groups (see Method section and Supporting Information for details). This conjugation strategy allows every bound Fn to retain full activity, a clear advantage over antibodies, which are often bound to the nanowire surface *via* amine containing residues, randomly distributed on the antibody surface.[2−7] Moreover, our Fn can also be easily configured with other functional groups, such as azides[13,14] or cyclopentadienes,[15] that are useful in bioconjugation.

Details of device fabrication, functionalization, and experimental conditions used here can be found in the Method section. Briefly, In_2O_3 nanowires were grown *via* a laser ablation CVD method on a Si/SiO_2 substrate, following a well-established procedure in our laboratory.[16−19] The nanowires were suspended in isopropyl alcohol and deposited onto another Si/SiO_2 substrate. The position of the source and drain (S−D) electrodes was defined by photolithography, with channel length and width of 2.5 and 780 μm, respectively. Metal deposition on the prepatterned surface followed by lift-off completed the device fabrication. Immediately after cleaning, the nanowire devices were submerged in a 0.1 mM aqueous solution of 6-phosphonohexanoic acid followed by baking in inert atmosphere, resulting in the binding of the phosphonic acid to the surface of the In_2O_3 NWs. The S−D contacts were then wired to a custom-made printed circuit board, and a mixing cell was assembled on the device chip (Supporting Information, Figure S3). This mixing cell was used to deliver and handle all the chemical reagents necessary to complete the surface modification and all the buffer solutions during active measurements.

We have then measured the device characteristics utilizing a liquid gate electrode[20] while using the above-described set up. Our In_2O_3 NW FET devices exhibit excellent transistor behavior in 0.01× phosphate buffered saline (PBS) solution. The linear behavior of the source/drain current *versus* source/drain voltage ($I_{ds}-V_{ds}$) curves at $V_{ds,} \leq 0.08$ V (Figure 1b) suggests good contact between the nanowires and source/drain electrodes. Strong gate dependence was also observed for a typical device, as shown by the I_{ds} *versus* liquid gate voltage ($I_{ds}-V_g$) curves shown in linear (red curve) and logarithmic scale (blue) in Figure 1c. The on/off ratio and transconductance were ~4.6×10^3 and ~3.6 μS, respectively. These results confirm the stability of our devices under active measurement conditions.

Further surface modification of the nanowires conferred our devices with the desired biological recognition properties. The carboxylic acid functional groups on the NW surface were activated with EDC and the activated COOHs were allowed to react with BMPH, resulting in the formation of a NW surface reactive toward the unique thiol present on the Fibronectin probe molecule. The functionalized devices were stored submerged in 1× PBS at 4 °C.

The normalized electrical response of an Fn-modified nanowire device is shown in Figure 2a−c, where we have plotted I_{ds} divided by the I_{ds} at $t = 0$ s, referred to as I/I_0. The device was operated at $V_{ds} = -200$ mV and $V_g = -100$ mV. Under such experimental conditions, a baseline signal was quickly established in pure 0.01× PBS buffer, as indicated in Figure 2a. We note that the leakage current between source and drain through the buffer is negligible compared to the conduction through nanowires (see Supporting Information). A shift in the baseline level is often observed when transitioning from pure buffer to protein-rich buffer, attributed to nonspecific binding interactions of proteins with the nanowire device. These nonspecific binding phenomena, if not adequately mitigated, may lead to false positive results. Passivating regions of the device that are subject to nonspecific binding with a "blocking agent" (typically BSA or Tween 20), as traditionally used in bioanalytical assays such as ELISA,[21,22] is technique useful to minimize false positives during active measurements. We have employed BSA as "blocking agent" for our nanowire devices including the source−drain electrodes. Aliquots of a 10 mg/mL solution of BSA were used to increase the protein concentration of the buffer in contact with the nanowires. After each BSA addition, the baseline re-equilibrated to a lower value of S−D current, as shown in Figure 2a,b. Saturation of nonspecific binding sites was achieved at 40 μM concentration of BSA, as indicated in Figure 2b. We note that BSA passivation is widely employed in many standard detection techniques such as ELISA; however, it may be possible that the BSA passivation step can be eliminated by increasing the surface coverage of Fn. The baseline stability in a protein-rich medium was then tested by increasing the BSA concentration by 10% (4 μM) (shown with a black arrow in Figure 2c). The device showed no significant response, which confirmed that sites for nonspecific binding were blocked. The conductance of the device rapidly decreased (4%) upon exposing the nanowire sensor to a solution containing 0.6 nM of N protein in 44 μM BSA. We further tested the response of our devices to higher N-protein concentrations. N-protein solutions were prepared by successive additions of small aliquots of a 100 ± 30 nM stock solution of N-protein in 0.01× PBS containing 44 μM BSA. When the N protein concentration was progressively increased to 2, 5, and 10 nM, we observed a consistent decrease in device conductance of 12%, 22%, and 31%, respectively, relative to the baseline. The pI of In_2O_3 is ~8,[23] and the pI of N protein is ~10,[24] while the PBS buffer we used had pH = 7.4. The pI of the N protein indicates that our target analyte possesses a net positive charge under our measurement conditions. However, some regions of N proteins are locally negatively charged, such as the C-terminus of N protein, which is rich in serine groups (pI ≈ 5).[25] The pI of In_2O_3 indicates that the surface of our In_2O_3 nanowires is positively charged. Thus, it might be possible that the positive charges on In_2O_3 nanowires attract the negatively charged regions of N protein captured on the nanowire surface. These serine residues could induce a chemical gating effect on the nanowires, causing a decrease in the conductance of our device. Other non-negligible contributions to the sensing mechanism could come from an increase of the carrier scattering due to the binding of N protein. We note that the sensing mechanism for nanobiosensors is still a topic of intense debate in the literature[26−30] and it is currently under intensive investigations in our research group.

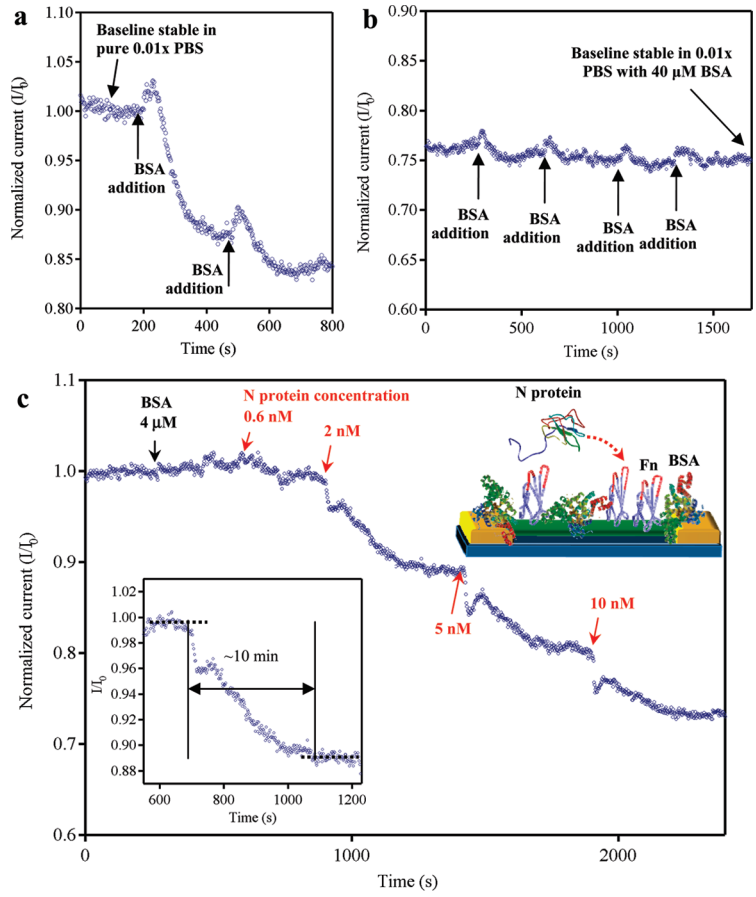

Figure 2. Normalized electrical output (I/I_0) *versus* time of a single operating device. (a−b) Response curves to passivation upon addition of successive aliquots of BSA. Upon increasing the concentration of BSA (from pure 0.01× PBS), the baseline re-equilibrates at lower values of S−D current until stability is ultimately reached at 40 μM BSA, in 0.01× PBS. (c) Response for a nanowire device functionalized with Fn. The red arrows indicate the times when the solution was raised to a given concentration of N protein. The inset on the right side is the configuration of our device during active sensing measurements. BSA protein was used to block sites for nonspecific binding. The Fn probe molecule was then used to specifically capture the target N protein. The inset on the left side is to show the plateau and the definition of response time.

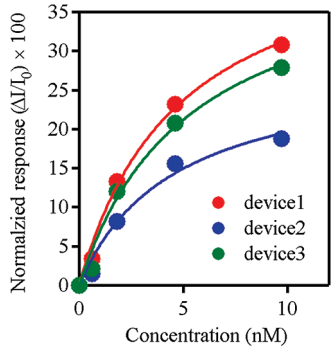

Figure 3. Normalized response from three devices *versus* concentration of N protein (dots). These plots can be fitted using a Langmuir isotherm model (solid line).

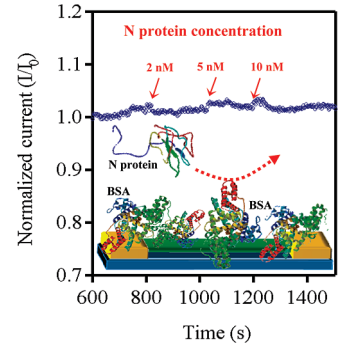

Figure 4. A control device without the Fn capture probe does not respond to the presence of N protein.

We have defined the response time to be the time necessary to achieve equilibrium after a change in the concentration of the N protein. Under our active measurement conditions, the response time turned out to be in the order of ~10 min as shown in Figure 2c inset for one measurement. This response time can be considered relatively short when compared to the time required to produce a signal using other diagnostic technologies such as ELISA (~hours),[31] which requires multistep analysis. Thus, while detecting the N protein in the nanomolar range can also be achieved using current immunological clinical tests, our nanowire sensors offer additional advantages such as label free detection and a comparatively short response time.

Three devices were tested in parallel, and all the devices showed a quantitatively similar concentration dependence for their response. Plots of sensor response *versus* N-protein concentration for these three devices are shown in Figure 3 (dots), confirming the reproducibility of the results. These plots were fitted using a conventional Langmuir isotherm model[32,33] (solid line), and these fits were used to estimate the dissociation constant of Fn to the N protein. In applying this model, we assumed that the response of the sensor is proportional to the number of captured molecules on the sensor surface, such that $I/I_0 \propto$ Fn surface coverage. The following equation was used to describe the concentration dependence of our sensor response:

$$\Delta I/I_0 = A\frac{\alpha n}{1 + \alpha n} \quad (1)$$

where A is a coefficient that converts surface coverage into electrical response, α is a constant, and n is the concentration of N protein. The values of A and α were determined using the least-squares method to give the best fit to the experimental values. The dissociation constant was estimated by calculating the solution of n in the following equation:

$$\theta = \Delta I/I_0\frac{1}{A} = \frac{\alpha n}{1 + \alpha n} = 0.5 \quad (2)$$

where θ is the percentage coverage of the surface, since the definition of dissociation constant is an analyte concentration when half of the sites are occupied. Application of this analytical model yields a dissociation constant of 4.9 ± 0.4 nM, which is close to the value of the dissociation constant (K_D = 3.3 nM) obtained from measurements of surface plasmon resonance (SPR).[12] The close match of the dissociation constant illustrates the validity of our assumption and the Langmuir isotherm model. The small difference may come from the fact that the measurements were done in buffers with different ionic strengths (0.01× PBS for nanobiosensor and 1× PBS for SPR).

We conducted further experiments to confirm the role of Fn as a selective capture probe. A nanowire surface, previously activated for bioconjugation, was treated with 2-mercaptoethanol, prior to Fn. The Fn capture probe is not expected to bind to the nanowire surface coated with 2-mercaptoethanol moieties, and thus this device should not specifically recognize the N protein. A baseline was established for this device after saturation of any site for nonspecific binding with a 40 μM solution of BSA as for the device with Fn (Figure S5). This device was then sequentially exposed to a 2, 5, and 10 nM solution of N protein, while still in the presence of 40 μM BSA. (Figure 4) We did not observe any significant responses, in sharp contrast to the response observed when we used a device functionalized with Fn, confirming that our Fn-based capture probe can selectively capture the N protein.

In conclusion, we have demonstrated that AMPs can be employed as capture agents in nanobiosensors. Sensors based on In_2O_3 nanowires were modified with a fibronectin-based binding agent that can selectively detect the SARS biomarker N protein. The N protein was detected at a sensitivity comparable to current immunological detection methods (subnanomolar concentration), but obtained within shorter time and without the aid of labeled reagents. We believe that nanowire biosensor devices functionalized with engineered proteins (evolved to possess elevated affinity toward target molecules) can have important potential applications

ranging from disease diagnosis to homeland security. This report also demonstrates the potential for nanobiosensors to be used as an accurate, convenient, and rapid tool to measure the dissociation constants for biological complex systems, such as antibody−antigen, protein−ligand, oligonucleotides, *etc.*

METHOD

Materials. Phosphate buffer saline (PBS, pH = 7.40, 10 mM phosphates, 137 mM NaCl, 2 mM KCl) was purchased from Mediatech Inc. Water was of high purity (HPLC grade). [(2-*N*-Morpholino) ethanesulfonic acid] buffer (MES buffer, 100 mM, pH = 5.2) was purchased from Fluka. (1-Ethyl-3-[3-dimethylaminopropyl]carbodiimide hydrochloride) (EDC) was purchased from Aldrich. *N*-[β-Maleimidopropionic acid] hydrazide, trifluoroacetic acid salt (BMPH) was purchased from Pierce. 6-Phosphohexanoic acid was purchased from Aldrich. Bovine serum albumin (BSA) was purchased from Sigma. Aqueous solution of 0.01% Au nanoparticles (mean diameter: 9.6 nm) were purchased from BBInternational. Indium arsenide was purchased from Alfa Aesar. Stock solutions of Fibronectin (1 μM in 1× PBS buffer) and N protein (200 nM in 1× PBS buffer) were provided by Prof. Ren Sun's research group. The N protein solution was buffer exchanged to 0.01× PBS before use with a NAP-5 column (Amersham Scientific). We note that during buffer exchange the concentration of the N protein is lowered due to about 2-fold dilution. We estimate the concentration of N protein in 0.01× PBS to be 100 nM with an error bar of ±30%.

Device Fabrication. In_2O_3 nanowires were grown *via* a laser ablation CVD method on a Si/SiO_2 substrate, following a well-established procedure in our laboratory.[4,17] Briefly, a stock aqueous solution of Au nanoparticles, with a diameter of about 10 nm, was obtained by a 1:10 dilution of the purchase solution in isopropyl alcohol. A veil of this diluted Au nanoparticle solution was allowed to dry on a Si/SiO_2 surface (typical size: 1−2 cm^2), resulting in a uniform surface coating of Au nanoparticles. These nanoparticles were then employed as a catalyst for the laser ablation promoted growth of indium oxide nanowires, using InAs as a source of In. Details of the nanowire growth are described elsewhere.[16,18,19] The as-grown nanowires were suspended in isopropyl alcohol by sonication and this suspension was deposited onto another Si/SiO_2 substrate (typically on a 3'' Si wafer with a surface coverage of 1 nanowire per 100 μm^2). The position of the source and drain (S−D) electrodes was defined by photolithography. The S−D electrodes were designed to have an interdigitated interface at the semiconductor channel, leading to FETs with channel length and width of 2.5 and 780 μm, respectively. Metal deposition (5 nm of Ti and 50 nm of Au) on the prepatterned surface followed by lift-off completed the device fabrication.

Surface Functionalization. ***In_2O_3 NW Device Cleaning Procedure.*** In_2O_3 NW devices were submerged for 5 min each in boiling tetrachloroethylene, acetone, ethanol, and water. The NW devices were rinsed with ethanol, dried with nitrogen, placed in a ozone/UV chamber for 8−10 min, and then submerged in hot water (80−90 °C) for 5 min.

Attachment of the Fibronectin Probe Molecule. The attachment of the Fibronectin probe molecules is schematically illustrated in Figure S2. Immediately after cleaning, the nanowire devices were submerged in a 0.1 mM aqueous solution of 6-phosphonohexanoic acid for 16 h at room temperature, resulting in the binding of the phosphonic acid residue to the surface of the In_2O_3 NWs (i). These devices were baked at 125 °C under nitrogen for 2 h. These devices were then wired on a custom-made printed circuit board and a mixing cell was assembled on the device chip (Figure S3). This mixing cell was used to deliver and handle all the chemical reagents necessary for surface modification and all the buffer solutions during active measurements. The carboxylic acid functional groups on the NW surface were activated by placing in the mixing cell a 50 mM solution of EDC in MES buffer and allowing the activated COOHs to react with BMPH (present in the same solution at 5 mM concentration) for 60−90 min (ii). Unreacted, EDC-activated carboxyl groups were quenched with a 50 mM solution of ethanolamine (ii). This resulted in the formation of a NW surface reactive toward the unique thiol present on the Fibronectin probe molecule. This EDC/BMPH solution was removed from the mixing cell by progressive dilution with PBS buffer. A solution containing about 200 nM of Fn in 1× PBS (along with 1 equiv of TCPE) was allowed to react with the NW surface, overnight, at 4 °C (iii). The unreacted maleimide groups were quenched with the addition of 10 uL of a 50 mM solution of 2-mercaptoethanol and allowed to react for 10−15 min (iii). This Fn solution was replaced with 1× PBS by progressive dilutions and the functionalized devices were stored submerged in 1× PBS at 4 °C.

Acknowledgment. We acknowledge financial support from the Whittier Foundation and the National Institute of Health.

Supporting Information Available: Engineered Fibronectin, surface functionalization, experimental setup, measurement of leakage current, absolute response, and a control experiment. This material is available free of charge *via* the Internet at http://pubs.acs.org.

REFERENCES AND NOTES

1. Cui, Y.; Wei, Q. Q.; Park, H. K.; Lieber, C. M. Nanowire Nanosensors for Highly Sensitive and Selective Detection of Biological and Chemical Species. *Science* **2001**, *293*, 1289–1292.
2. Patolsky, F.; Zheng, G.; Lieber, C. M. Nanowire Sensors for Medicine and the Life Sciences. *Nanomedicine* **2006**, *1*, 51–65.
3. Stern, E.; Klemic, J. F.; Routenberg, D. A.; Wyrembak, P. N.; Turner-Evans, D. B.; Hamilton, A. D.; LaVan, D. A.; Fahmy, T. M.; Reed, M. A. Label-Free Immunodetection with Cmos-Compatible Semiconducting Nanowires. *Nature (London)* **2007**, *445*, 519–522.
4. Li, C.; Curreli, M.; Lin, H.; Lei, B.; Ishikawa, F. N.; Datar, R.; Cote, R. J.; Thompson, M. E.; Zhou, C. W. Complementary Detection of Prostate-Specific Antigen Using In_2O_3 Nanowires and Carbon Nanotubes. *J. Am. Chem. Soc.* **2005**, *127*, 12484–12485.
5. Curreli, M.; Zhang, R.; Ishikawa, F. N.; Chang, H.-K.; Cote, R. J.; Zhou, C.; Thompson, M. E. Real-Time, Label-Free Detection of Biological Entities Using Nanowire-Based FETs. *IEEE Trans. Nanotechnol.* **2008**, *7*, 651–667.
6. Gruner, G. Carbon Nanotube Transistors for Biosensing Applications. *Anal. Bioanal. Chem.* **2006**, *384*, 322–335.
7. Allen, B. L.; Kichambare, P. D.; Star, A. Carbon Nanotube Field-Effect-Transistor-Based Biosensors. *Adv. Mater.* **2007**, *19*, 1439–1451.
8. Bunimovich, Y. L.; Shin, Y. S.; Yeo, W. S.; Amori, M.; Kwong, G.; Heath, J. R. Quantitative Real-Time Measurements of DNA Hybridization with Alkylated Nonoxidized Silicon Nanowires in Electrolyte Solution. *J. Am. Chem. Soc.* **2006**, *128*, 16323–16331.
9. Binz, H. K.; Amstutz, P.; Pluckthun, A. Engineering Novel Binding Proteins from Nonimmunoglobulin Domains. *Nat. Biotechnol.* **2005**, *23*, 1257–1268.
10. Binz, H. K.; Pluckthun, A. Engineered Proteins as Specific Binding Reagents. *Curr. Opin. Biotechnol.* **2005**, *16*, 459–469.
11. Zakhartchouk, A. N.; Viswanathan, S.; Mahony, J. B.; Gauldie, J.; Babiuk, L. A. Severe Acute Respiratory Syndrome Coronavirus Nucleocapsid Protein Expressed by an Adenovirus Vector Is Phosphorylated and Immunogenic in Mice. *J. Gen. Virol.* **2005**, *86*, 211–215.
12. Liao, H. I.; Olson, C. A.; Ishikawa, F. N.; Curreli, M.; Chang, H.-K.; Thompson, M. E.; Zhou, C.; Roberts, R. W.; Sun, R., to be submitted for publication.

13. Bunimovich, Y. L.; Ge, G.; Beverly, K. C.; Ries, R. S.; Hood, L.; Heath, J. R. Electrochemically Programmed, Spatially Selective Biofunctionalization of Silicon Wires. *Langmuir* **2004**, *20*, 10630–10638.
14. Rohde, R. D.; Agnew, H. D.; Yeo, W. S.; Bailey, R. C.; Heath, J. R. A Non-Oxidative Approach toward Chemically and Electrochemically Functionalizing Si(111). *J. Am. Chem. Soc.* **2006**, *128*, 9518–9525.
15. Yousaf, M. N.; Houseman, B. T.; Mrksich, M. Using Electroactive Substrates to Pattern the Attachment of Two Different Cell Populations. *Proc. Natl. Acad. Sci. U.S.A.* **2001**, *98*, 5992–5996.
16. Liu, F.; Bao, M.; Wang, K. L.; Li, C.; Lei, B.; Zhou, C. One-Dimensional Transport of In_2O_3 Nanowires. *Appl. Phys. Lett.* **2005**, *86*, 213101–213103.
17. Curreli, M.; Li, C.; Sun, Y. H.; Lei, B.; Gundersen, M. A.; Thompson, M. E.; Zhou, C. W. Selective Functionalization of In_2O_3 Nanowire Mat Devices for Biosensing Applications. *J. Am. Chem. Soc.* **2005**, *127*, 6922–6923.
18. Lei, B.; Li, C.; Zhang, D.; Tang, T.; Zhou, C. Tuning Electronic Properties of In_2O_3 Nanowires by Doping Control. *Appl. Phys. A: Mater. Sci. Process.* **2004**, *79*, 439–442.
19. Li, C.; Zhang, D.; Han, S.; Liu, X.; Tang, T.; Lei, B.; Liu, Z.; Zhou, C. Synthesis, Electronic Properties, and Applications of Indium Oxide Nanowires. In *Molecular Electronics III*; New York Academy of Sciences: New York, 2003; Vol. 1006, pp 104−121.
20. Rosenblatt, S.; Yaish, Y.; Park, J.; Gore, J.; Sazonova, V.; McEuen, P. L. High Performance Electrolyte Gated Carbon Nanotube Transistors. *Nano Lett.* **2002**, *2*, 869–872.
21. Stadtherr, K.; Wolf, H.; Lindner, P. An Aptamer-Based Protein Biochip. *Anal. Chem.* **2005**, *77*, 3437–3443.
22. Ausubel, F. M.; Brent, R.; Kingston, R. E.; Moore, D. D.; Seidman, J. G.; Smith, J. A.; Struhl, K. *Current Protocols in Molecular Biology*; John Wiley and Sons Inc.: Hoboken, NJ, 2007.
23. Kosmulski, M. Pristine Points of Zero Charge of Gallium and Indium Oxides. *J. Colloid Interface Sci.* **2001**, *238*, 225–227.
24. Mark, J.; Li, X. G.; Cyr, T.; Fournier, S.; Jaentschke, L.; Hefford, M. A. Sars Coronavirus: Unusual Lability of the Nucleocapsid Protein. *Biochem. Biophys. Res. Commun.* **2008**, *377*, 429–433.
25. Lai, M. M. C.; Cavanagh, D. The Molecular Biology of Coronaviruses. *Adv. Virus Res.* **1997**, *48*, 1–100.
26. Nair, P. R.; Alam, M. A. Screening-Limited Response of Nanobiosensors. *Nano Lett.* **2008**, *8*, 1281–1285.
27. Heller, I.; Janssens, A. M.; Mannik, J.; Minot, E. D.; Lemay, S. G.; Dekker, C. Identifying the Mechanism of Biosensing with Carbon Nanotube Transistors. *Nano Lett.* **2008**, *8*, 591–595.
28. Stern, E.; Wagner, R.; Sigworth, F. J.; Breaker, R.; Fahmy, T. M.; Reed, M. A. Importance of the Debye Screening Length on Nanowire Field Effect Transistor Sensors. *Nano Lett.* **2007**, *7*, 3405–3409.
29. Tang, X. W.; Bansaruntip, S.; Nakayama, N.; Yenilmez, E.; Chang, Y. L.; Wang, Q. Carbon Nanotube DNA Sensor and Sensing Mechanism. *Nano Lett.* **2006**, *6*, 1632–1636.
30. Chen, R. J.; Choi, H. C.; Bangsaruntip, S.; Yenilmez, E.; Tang, X. W.; Wang, Q.; Chang, Y. L.; Dai, H. J. An Investigation of the Mechanisms of Electronic Sensing of Protein Adsorption on Carbon Nanotube Devices. *J. Am. Chem. Soc.* **2004**, *126*, 1563–1568.
31. Crowther, J. R. *Elisa: Theory and Practice*; Humana Press: New York, 1995.
32. Langmuir, I. The Constitution and Fundamental Properties of Solids and Liquids Part I Solids. *J. Am. Chem. Soc.* **1916**, *38*, 2221–2295.
33. Halperin, A.; Buhot, A.; Zhulina, E. B. On the Hybridization Isotherms of DNA Microarrays: The Langmuir Model and Its Extensions. *J. Phys. Condens. Matter* **2006**, *18*, S463−S490.

Label-Free, Electrical Detection of the SARS Virus N-Protein With Nanowire Biosensors Utilizing Antibody Mimics as Capture Probes

Fumiaki N. Ishikawa,[(a)] Hsiao-Kang Chang,[(a)] Marco Curreli,[(b)] Hsiang-I Liao,[(d)] C. Anders Olson,[(b)] Po-Chiang Chen,[(a)] Rui Zhang,[(b)] Richard W. Roberts,[(b)] Ren Sun,[(d)] Richard J. Cote,[(c)] Mark E. Thompson,[(b)]* Chongwu Zhou[(a)]*

Departments of [(a)]Electrical Engineering,[(b)]Chemistry, and [(c)]Pathology, University of Southern California, Los Angeles, CA 90089

Department of [(d)]Molecular and Medical Pharmacology, University of California Los Angeles, Los Angels, CA 90095

Supporting Information

Supporting Information Available: Engineered Fibronectin, surface functionalization, experimental setup, measurement of leakage current, absolute response, and a control experiment.

Table of Contents

Engineered Fibronectin

The design, evolution, and characterization of our Fibronectin (Fn) probe is described in details elsewhere.[1] It is worthy to note that our Fn was engineered in such a way to possess a single cystine in the protein, placed at the N' terminus of the polypeptide chain, as shown in Figure S1. This unique cystine was used as anchoring site for the attachment of Fn to the NW surface. Using this strategy, Fn immobilization on the nanowires occurs away from the binding region so the probe maintains an active configuration. Our Fn can also be configured with other functional groups useful in bioconjugation such as an azide or a cyclopentadiene.[2]

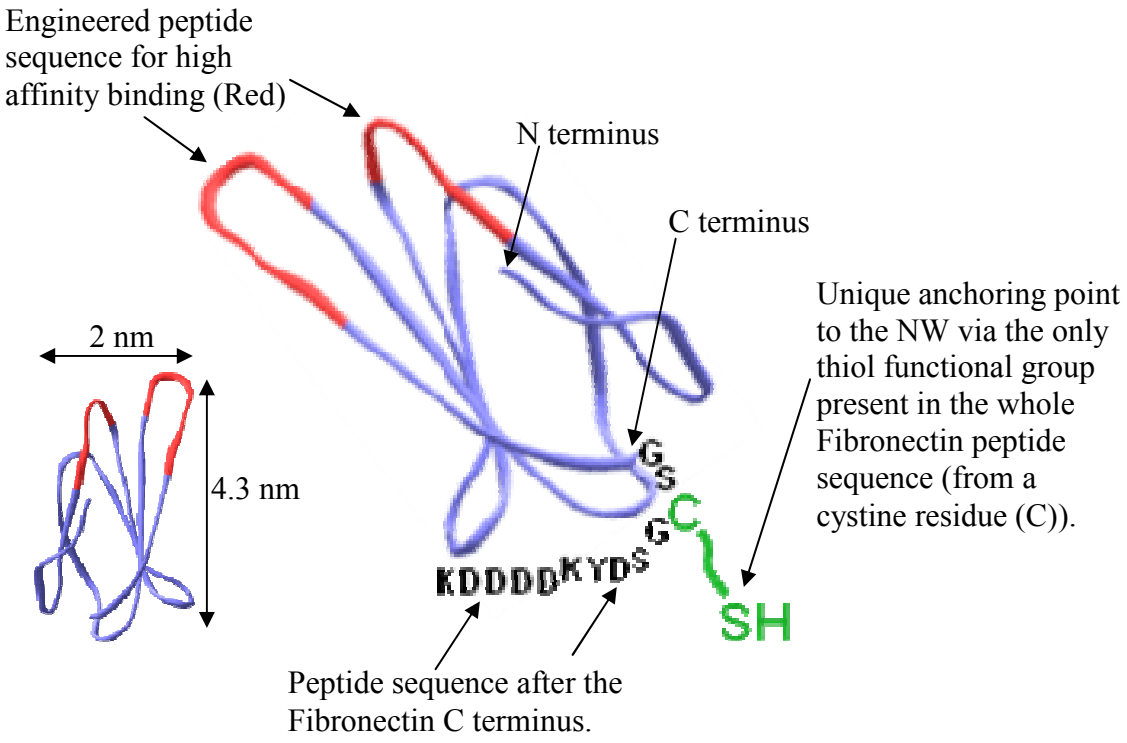

Figure S1. Ribbon structure of our engineered Fibronectin (Fn). The peptide sequence after the Fn C terminus is "spelled out" to show the position of our selective attachment point to the NW surface.

Surface functionalization

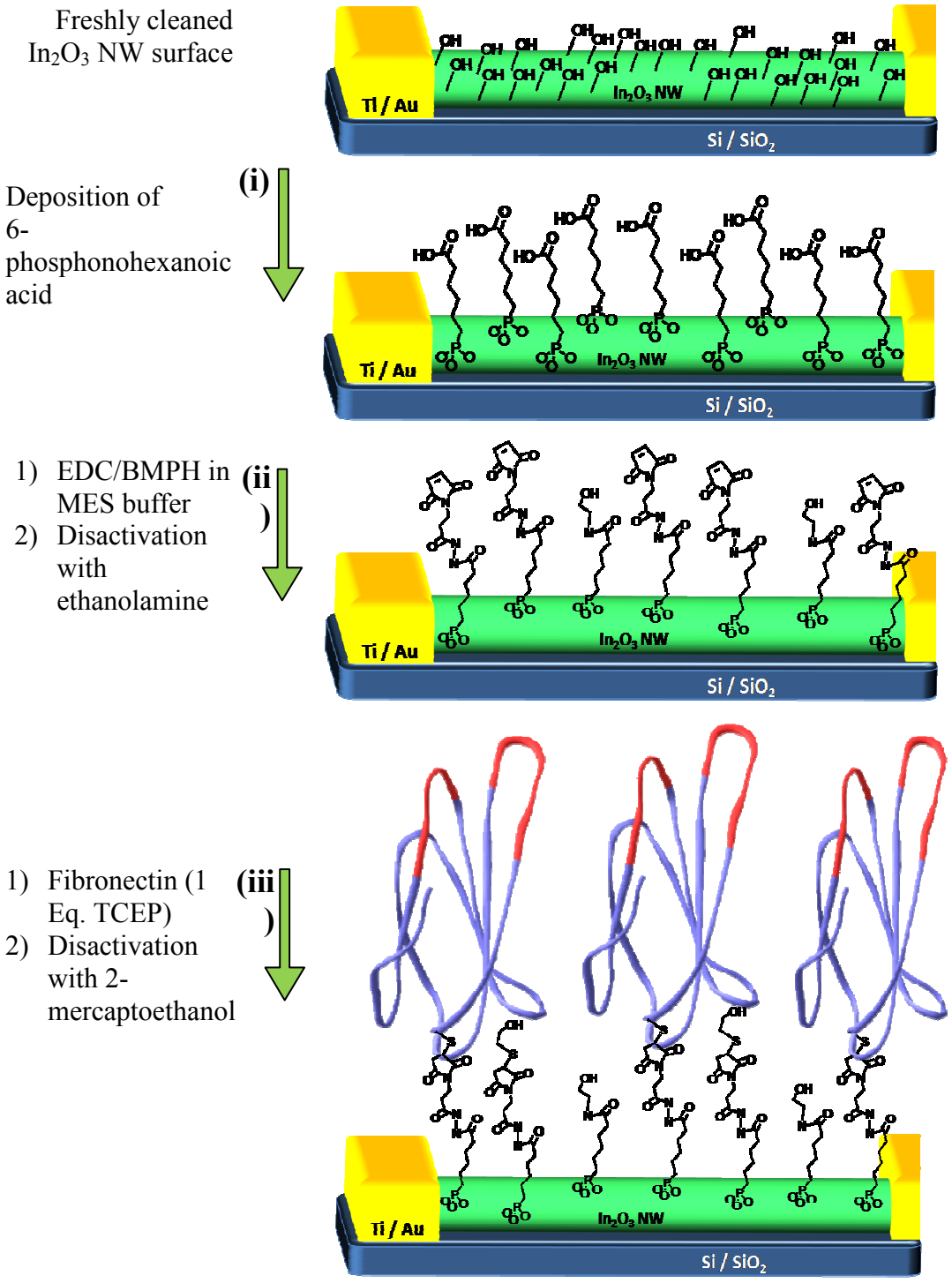

Figure S2. Surface modification of our In_2O_3 nanowire devices resulting in the covalent immobilization of the Fibronectin probe on the nanowires.

Experimental setup diagram

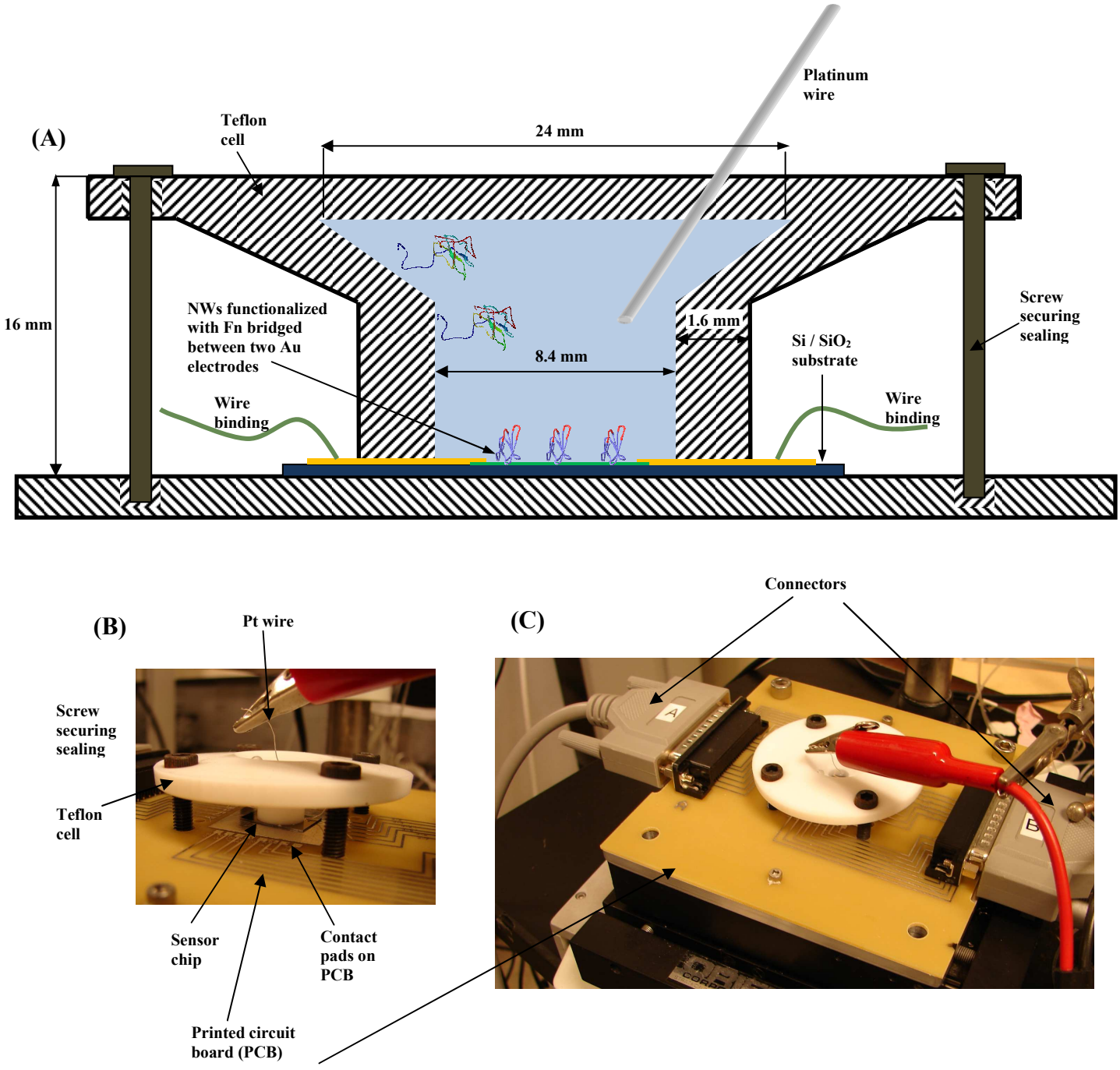

Fig. S3. Details and components are indicated in the figures. (A) Cross-section schematic diagram of the setup used for real time N protein sensing. This diagram is not on scale; the nanosensor device is shown enlarged for clarity with respect to the rest of the set up. (B) A side view of such setup. (C) A top-view photograph of the setup showing the Teflon cell atop a circuit board.

Leakage current between the source and drain electrode through the buffer

To determine the leakage through the aqueous solution, we measured the current from control devices without nanowires between the source and drain electrodes. Figure S4 plots the sensing response of a device with nanowires and a control device without nanowires, and one can clearly see that the leakage is negligible compared to the sensing signal. We note that the leakage current for the device without nanowires is typically around 1 pA, while the current for the device with nanowires is around 1.5 nA.

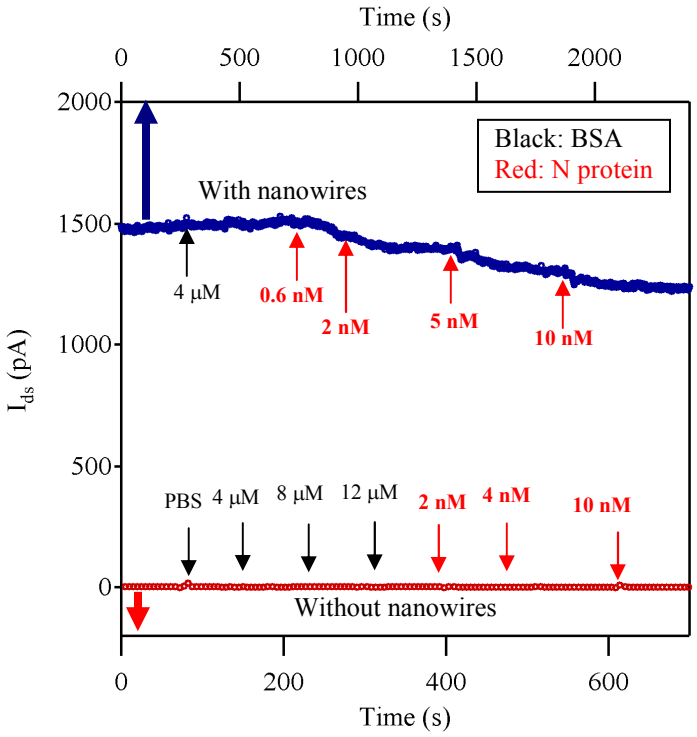

Figure S4. Plots of I_{ds} for a device with nanowires (blue) and a control device without nanowires (red) between the source and drain. The concentration of BSA and N protein is changed at the time indicated by the arrows.

Absolute responses for N protein sensing

Figure S5 shows the absolute response of three devices used in Figure 3 in the main text. It can be seen that, before normalization by the initial conductance, the response shows large device-to-device variation.

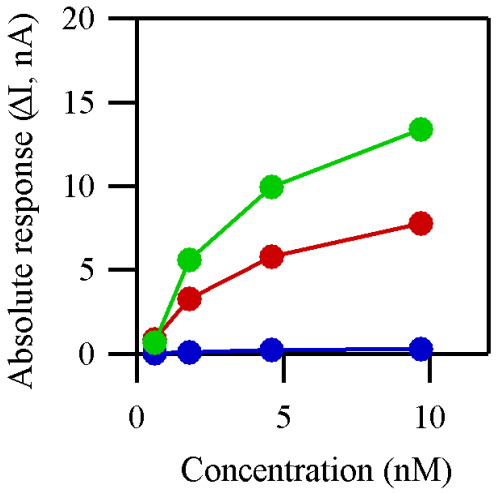

Figure S5. Absolute response of the three nanowire device used to detect the N protein. These are the same devices shown as relative response in Figure 3

Baseline for the control experiment to confirm the role of Fn

A device was functionalized according to steps (i), (ii), and (iii) outlined Fig. S2. The maleimide-surface-rich nanowire device was then treated with 2-mercaptoethanol prior to Fn immobilization (step (iv)). With all the binding sites blocked with 2-mercaptoethanol, the Fn capture probe is not expected to bind to the nanowire surface, and thus this device should not specifically recognize the N protein. A stable baseline was established for this device after saturation of any site for non-specific binding with a 40 μM solution of BSA (Fig. S6).

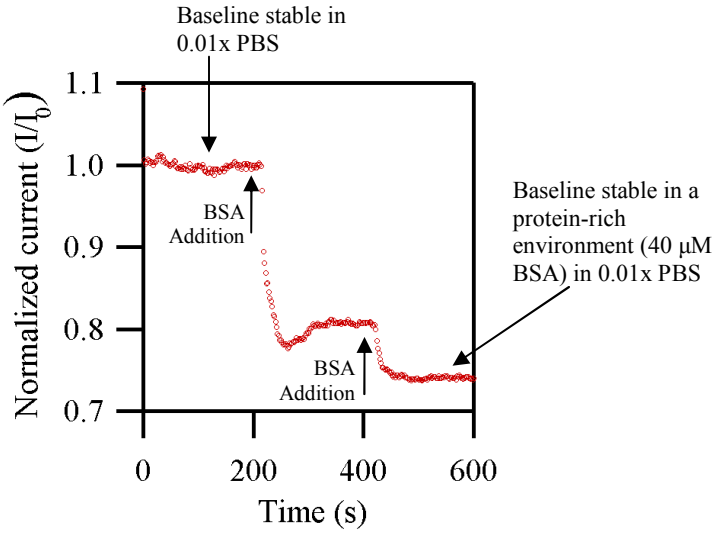

Figure S6. Establishing baseline in a protein-rich environment for the device passivated with 2-mercaptoethanol prior to Fn.

References

1 Liao, H. I.; Olson, C. A.; Ishikawa, F. N.; Curreli, M.; Chang, H.-K.; Thompson, M. E.; Zhou, C.; Roberts, R. W.; Sun, R., *in preparation*.

2 (a) Agnew, H.D.; Yeo, W.S.; Bailey; R.C.; Heath, J.R.; J. Am. Ch. Soc. 2006, 128, 9518-9525. (b) Bunimovich, Y. L.; Ge, G.; Beverly, K. C.; Ries, R. S.; Hood, L.; Heath, J. R. Langmuir 2004, 20, 10630-10638. (c) Yousaf, M.N.; Houseman, B. T.; Mrksich, M. PNAS 2001, 98, 5992-5996.